Subthreshold Behavior and Phenomenological Impedance of the Squid Giant Axon

A. MAURO, F. CONTI, F. DODGE, and R. SCHOR

From The Rockefeller University, New York 10021, Laboratory of Cybernetics and Biophysics of the CNR, Camogli, Italy, and the IBM Watson Research Center, Yorktown Heights, New York 10598

ABSTRACT The oscillatory behavior of the cephalopod giant axons in response to an applied current has been established by previous investigators. In the study reported here the relationship between the familiar "RC" electrotonic response and the oscillatory behavior is examined experimentally and shown to be dependent on the membrane potential. Computations based on the three-current system which was inferred from electrical measurements by Hodgkin and Huxley yield subthreshold responses in good agreement with experimental data. The point which is developed explicitly is that since the three currents, in general, have nonzero resting values and two currents, the "Na" system and the "K" system, are controlled by voltage-dependent time-variant conductances, the subthreshold behavior of the squid axon in the small-signal range can be looked upon as arising from phenomenological inductance or capacitance. The total phenomenological impedance as a function of membrane potential is derived by linearizing the empirically fitted equations which describe the time-variant conductances. At the resting potential the impedance consists of three structures in parallel, namely, two series RL elements and one series RC element. The true membrane capacitance acts in parallel with the phenomenological elements, to give a total impedance which is, in effect, a parallel R, L, C system with a "natural frequency" of oscillation. At relatively hyperpolarized levels the impedance "degenerates" to an RC system.

The subthreshold behavior of the axonal membrane, exemplified by the classical "electrotonus" of the myelinated nerve (Hermann, 1905; Hodgkin and Rushton, 1946; Davis and Lorente de Nó, 1947) and the "local response" and oscillatory behavior of the giant axon in the cephalopods, *Loligo* and *Sepia* (Hodgkin, 1938; Arvanitaki, 1939, 1941; Brink et al., 1946), have been studied by many investigators. In recent years, perhaps due to the advent of the microelectrode technique with its emphasis on large amplitude recordings, electrophysiologists have shown only moderate interest in the subthreshold be-

havior of the axonal membrane. In this communication we shall direct attention to the subthreshold behavior of the squid giant axon (see also Guttman, 1969; Sabah and Leibovic, 1969).

We shall first present the subthreshold behavior as displayed by excursions of the membrane potential of several millivolts in response to a constant current stimulus.[1] It will be seen that in general the response is oscillatory in character, and that the classical electrotonic response—the "RC" response—occurs, in fact, only at a unique level of the membrane potential and thus is a limiting case of the more general oscillatory behavior. Furthermore, it will be noted that the oscillatory behavior is maintained at a relatively constant frequency throughout the entire range of the subthreshold regime. This striking feature of the squid giant axon, namely, the existence of a "natural frequency" in the response of the membrane potential to an applied constant current, restricts the frequency range throughout which the axon can fire repetitively for suprathreshold currents. The narrow frequency range of repetitive firing is well-established experimentally (Hagiwara and Oomura, 1958) and stands in sharp contrast to the broad frequency range of firing seen in the sensory neuron; e.g., the slowly adapting crayfish stretch receptor (Eyzaguirre and Kuffler, 1955) or the eccentric cell in the ommatidium of *Limulus* (Fuortes, 1958).

Computed responses will then be presented based on the three-current system which was developed by Hodgkin and Huxley in 1952 (Hodgkin and Huxley, 1952) to describe the electrical responses observed in their study of the squid axon. It will be seen that the observed responses throughout the entire subthreshold regime are described successfully by a system of three ionic currents, two of which, the "sodium" and "potassium" currents, are mediated by voltage-dependent time-variant conductances and a third, the "leakage" current, by a linear time-invariant conductance, the electromotive force in each system being strictly time-invariant. The presentation of the results of the computations will serve a twofold purpose, namely, to supplement the subthreshold computations reported by Hodgkin and Huxley in 1952 (Hodgkin and Huxley, 1952) and by Huxley in 1959 (Huxley, 1959) and to extend the computations to the entire subthreshold regime.

Finally, in order to elucidate with maximum clarity the basis of the oscillatory behavior we shall treat in detail the subthreshold analysis for the condition of the axon in which only two currents exist, such that one, i.e. the "potassium system," is controlled by a time-variant conductance and the other, i.e. the "leakage current," by a time-invariant conductance. As has

[1] In this paper we shall consider only the nonpropagated response as is seen in a finite length of axon in which the applied current is uniform over the surface; i.e., the "space clamp" preparation. In a subsequent publication the experimental data and computations will be given for the propagated subthreshold response which is evoked in an "infinitely" extended axon with a point source of stimulating current.

been reviewed previously (Mauro, 1961), a fundamental phenomenological property of time-variant conductance underlies the observed small-signal[2] responses; i.e., phenomenological inductance or capacitance is manifested by time-variant conductance under certain conditions. In the case of the potassium time-variant conductance we shall see that if the resting current is different from zero a perturbing current will give rise to a small-signal response that will appear *as though* there were an inductance present when the resting current is outward, or a capacitance when the resting current is inward. At zero resting current, a condition that obtains when the membrane potential is equal to the emf of the potassium current, the system responds as a pure resistance.

Since in the squid giant axon a resting current exists in the potassium and the sodium system, it will be seen that both time-variant conductances act simultaneously to give a total "inductive-capacitive" response. The resulting total phenomenological impedance will be derived analytically from the empirical functions used by Hodgkin and Huxley to describe the measured time-variant conductances.[3]

METHODS

Freshly captured specimens of *Todarodes sagittatus*,[4] a giant squid found in the northern Mediterranean Sea, were used to obtain giant axon preparations. The giant axons were dissected free, cleaned, and mounted in approximately 45 min after decapitation of the animal. Details of the chamber have been described previously (Conti and Palmieri, 1968). It will suffice here to point out that the dissected length of axon was about 8 cm. By a suitable concentric internal electrode a 2 cm segment was observed under "space-clamped" conditions. The average diameter of the axons was about 400 μ. It is characteristic of this genus that the giant axon appears without branches, in sharp contrast to the axons of *Loligo*.

EXPERIMENTAL RESULTS

Small-Signal Responses A typical small-signal response of the membrane potential to a constant current is seen in Fig. 1. The current was adjusted to give a peak potential variation of less than 2 mv. With the onset of either a depolarizing or a hyperpolarizing current, the potential approaches the steady state through an oscillatory phase. Upon terminating the applied current, the response is characterized by an "overshooting" of the potential with respect to the resting potential. Note that the responses evoked by either a hyper-

[2] Subthreshold responses in the range of several millivolts will be referred to hereafter as small-signal responses.

[3] Similar expressions have been obtained by Chandler et al. (Chandler, FitzHugh, and Cole, 1962).

[4] This identification was made from color photographs by Dr. Frederick A. Aldrich, Marine Sciences Research Laboratory, Memorial University of Newfoundland, St. John's, Newfoundland, Canada. We thank him for his kind cooperation.

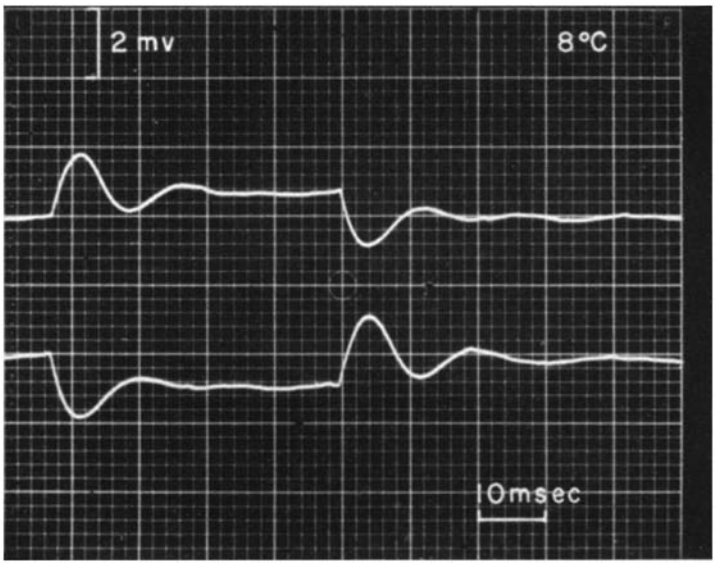

FIGURE 1. Small-signal response of space-clamped axon to a depolarizing and a hyperpolarizing constant current pulse. Axon at resting potential.

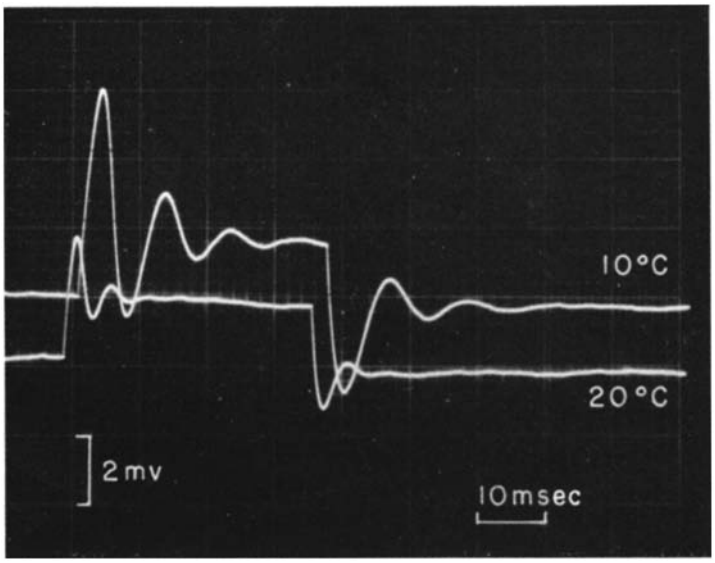

FIGURE 2. Small-signal response to a depolarizing current pulse. The recording was made on the same preparation, first, at room temperature, 20°C, and then at 10°C.

polarizing or a depolarizing current are virtually symmetrical indicating that the system is operating in the linear range.

Another striking feature of the oscillatory response is the marked dependence of the amplitude and frequency on temperature, such that an increase in

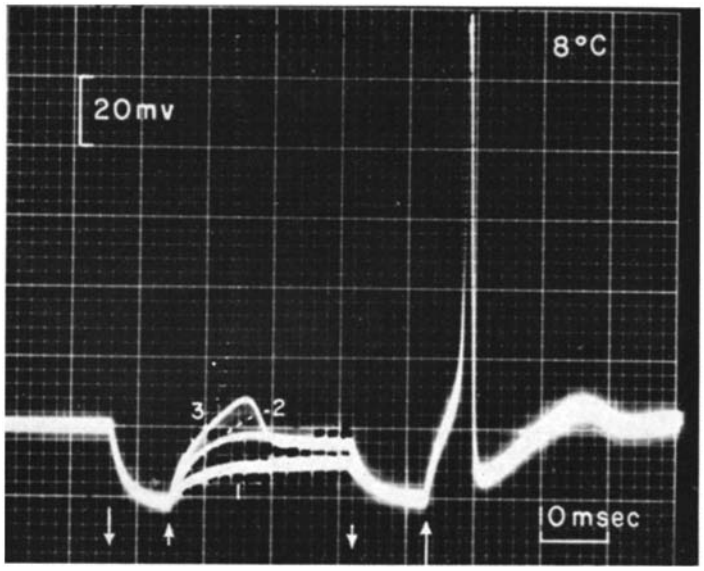

FIGURE 3. Small-signal response with the membrane hyperpolarized approximately 20 mv by an applied hyperpolarizing current (on and off indicated by large arrows). Small arrows indicate duration of test pulse. Responses designated 1, 2, and 3 occurred for three successively applied pulses. The current strength was increased in that order. Evoked spike is seen upon termination of hyperpolarizing current; i.e., "anodal break" response.

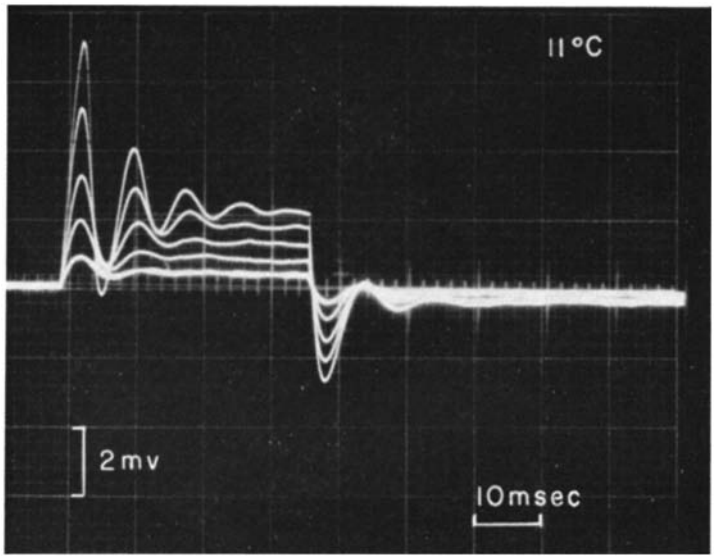

FIGURE 4. Oscillatory behavior recorded with successively applied constant current pulses of increasing magnitude. Note relative constancy in the frequency of sinusoidal waveform. Temperature 11°C.

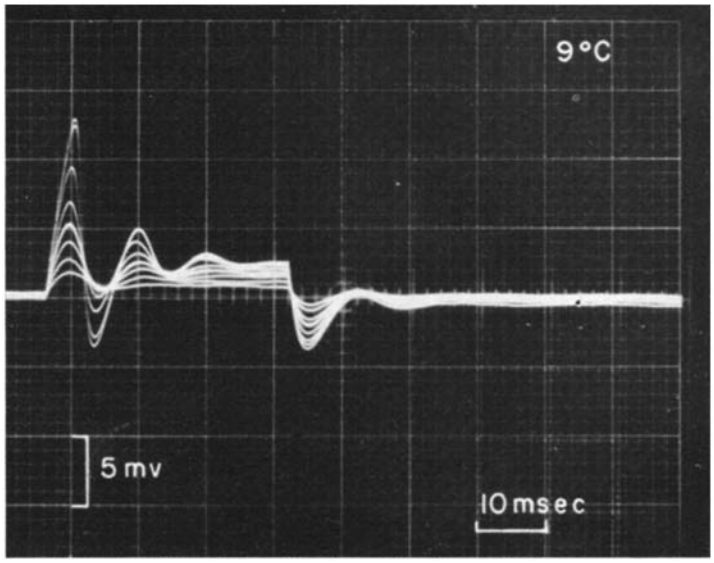

FIGURE 5. Results from another preparation as shown in Fig. 4. Temperature 9°C. The maximum current strength of pulse applied was barely subthreshold.

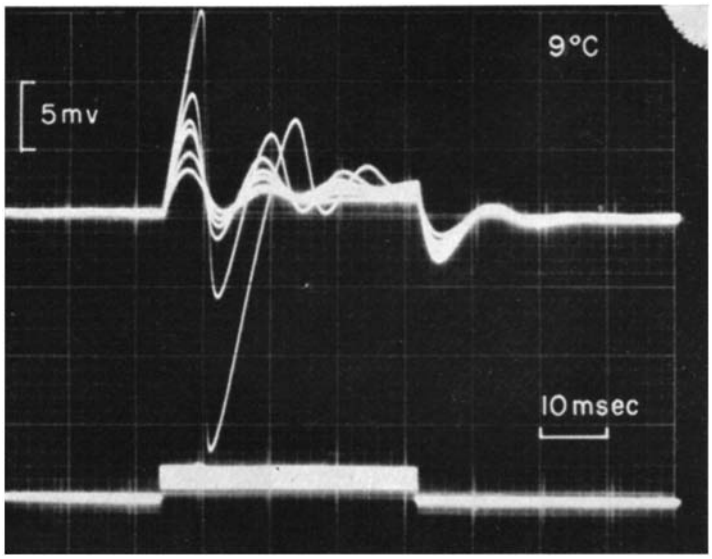

FIGURE 6. Responses throughout the entire subthreshold regime including a suprathreshold response (spike off scale) with the "undershoot" of the afterpotential and oscillatory recovery. Applied constant current pulses are recorded in the lower trace.

temperature brings about a decrease in the amplitude and the period of the response, as is seen in Fig. 2 for a small-signal recording observed on the same preparation at 10° and 20°C.

At a certain relatively hyperpolarized level of the membrane potential, the

small-signal response assumes the form of the typical RC response seen in many neuronal membranes. In Fig. 3 a recording is seen of the membrane potential in response to a pulse of depolarizing current which was applied 10 msec after the membrane had been hyperpolarized by approximately 20 mv. The first response, 1, evoked by a small current pulse, clearly is RC in character while the successive responses, 2 and 3, evoked by current pulses of increasing amplitudes display a damped oscillatory behavior.

Quasi–Small-Signal Responses At higher currents the augmented oscillatory response maintains its "sinusoidal" character over a wide range and,

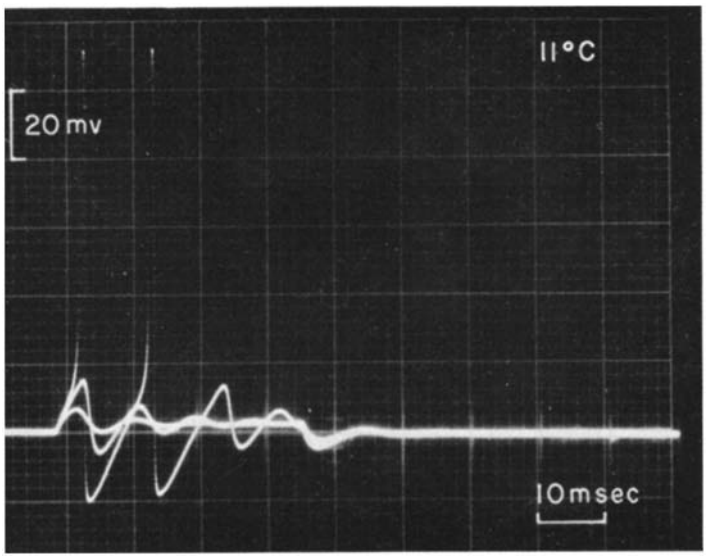

FIGURE 7. Subthreshold responses and onset of repetitive firing with two spikes evoked by suprathreshold current pulse. At a higher current this preparation gave an "infinite" train of spikes with a moderate increase in repetition rate relative to the subthreshold frequency of oscillation.

moreover, the frequency is relatively stable, increasing not more than 15% (see Figs. 4 and 5). It is convenient therefore for descriptive purposes to associate a natural frequency with the subthreshold response of the giant axon.

In Fig. 6 a recording is shown which includes the response to a threshold current (rheobase current). The upstroke of the spike is off scale. Note the marked undershooting and the oscillatory recovery at close to the natural frequency. In another experiment as seen in Fig. 7, a suprathreshold current was applied at a sufficient strength to evoke a second spike which is seen to arise from the second oscillation of the membrane potential. Currents of higher value gave trains of long duration at a frequency close to the subthreshold natural frequency.

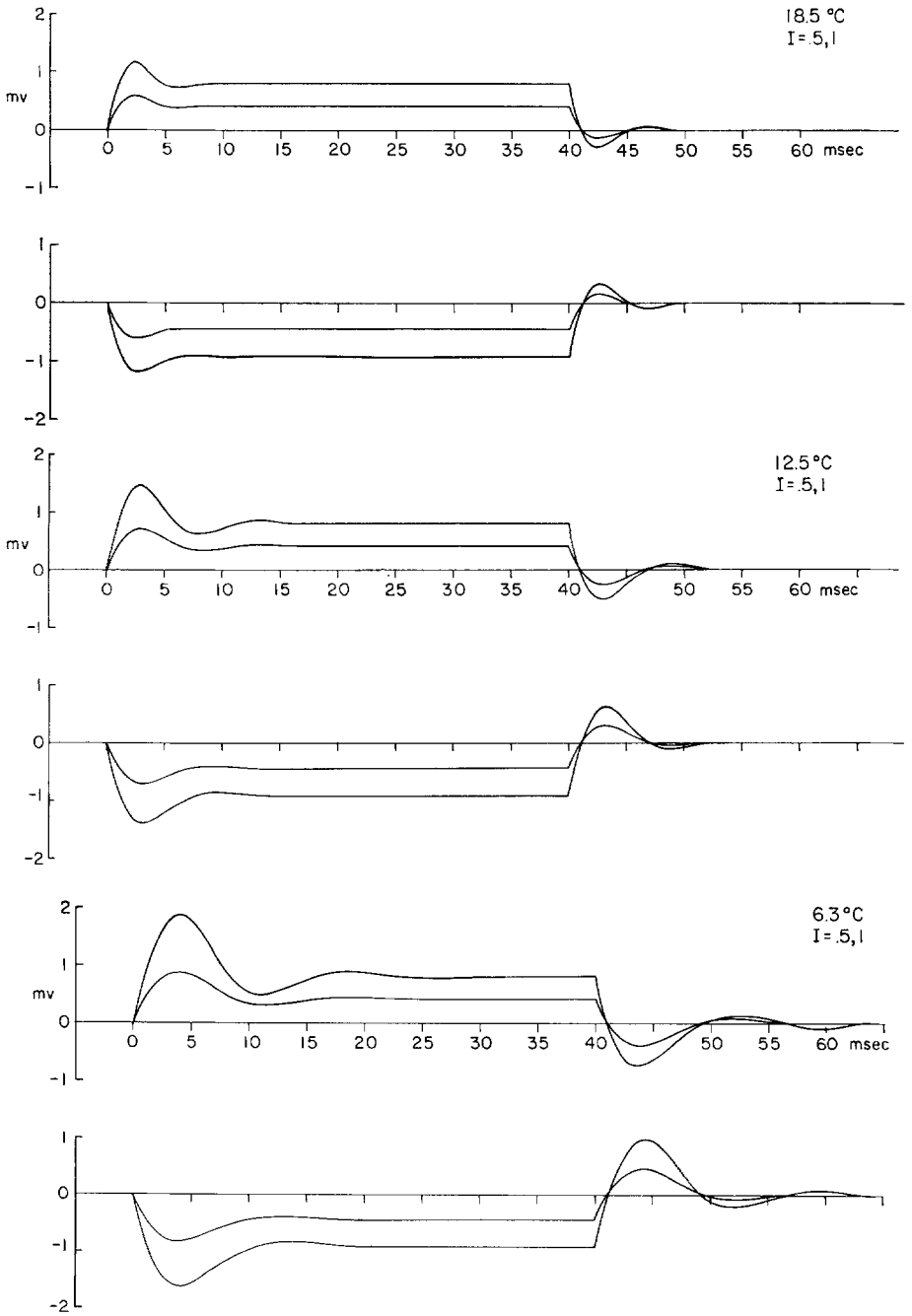

FIGURE 8. Computed small-signal responses of standard squid axon for a current pulse of 40 msec duration. Note the increase in the amplitude and period of the oscillation with decreasing temperature. The "off response" with a depolarizing and hyperpolarizing current pulse is also clearly evident. Current in μamp/cm^2.

Computed Responses

Before presenting the results of the computations based on the three-current system, it may be useful to summarize the essential points of the Hodgkin-Huxley analysis of the ionic currents in the squid giant axon. By applying steps of potential across the axonal membrane by means of a suitable electronic feedback arrangement and by manipulating certain experimental conditions, Hodgkin and Huxley were able to establish that at least three ionic currents

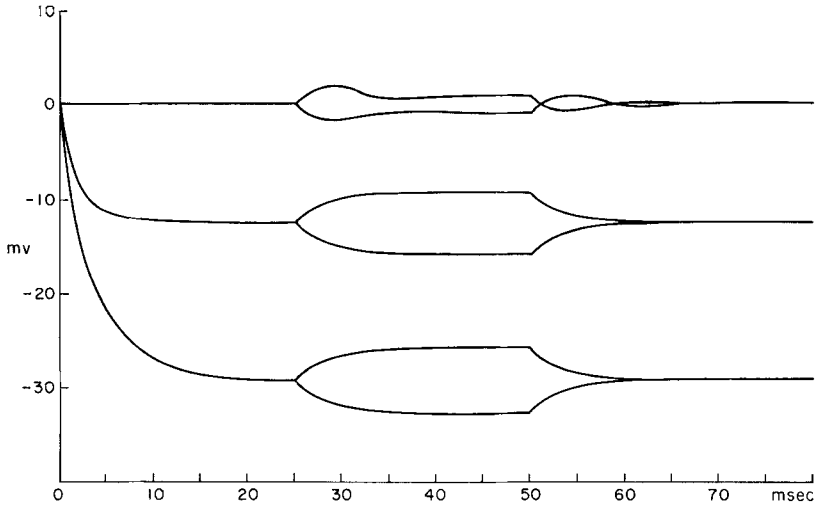

FIGURE 9. Computed small-signal response of standard squid axon at three levels of membrane potential, namely, resting potential ($V = 0$), -12 mv ($V = V_K$), and -29 mv, respectively. At each level the perturbing current pulse was 1 μamp/cm^2. The hyperpolarization of -12 mv and -29 mv required a hyperpolarizing current of -7 μamp/cm^2 and -12 μamp/cm^2, respectively. The transformation from an oscillatory response at the resting potential to an RC response at $V = -12$ mv is shown clearly. Temperature, 6.3°C.

exist in the squid axon membrane, two of which vary implicitly with time, i.e. are time-variant, and are markedly voltage-dependent, while the third is time-invariant and linear. The data also indicated that the respective electromotive forces are time-invariant. Thus by invoking the macroscopic law of current flow, namely, $I = g(V - E)$, wherein I, g, V, and E are the current, conductance, electric potential, and emf, respectively, they transformed the values of current vs. time to the corresponding values of the conductance vs. time. When the conductance data had been established, they succeeded in fitting an algebraic function to each of the two time-variant conductance curves. Finally, by invoking Kirchhoff's law of electric current with respect to the three ionic currents and the capacitive current in the membrane they obtained the electrical equation of state of the membrane.

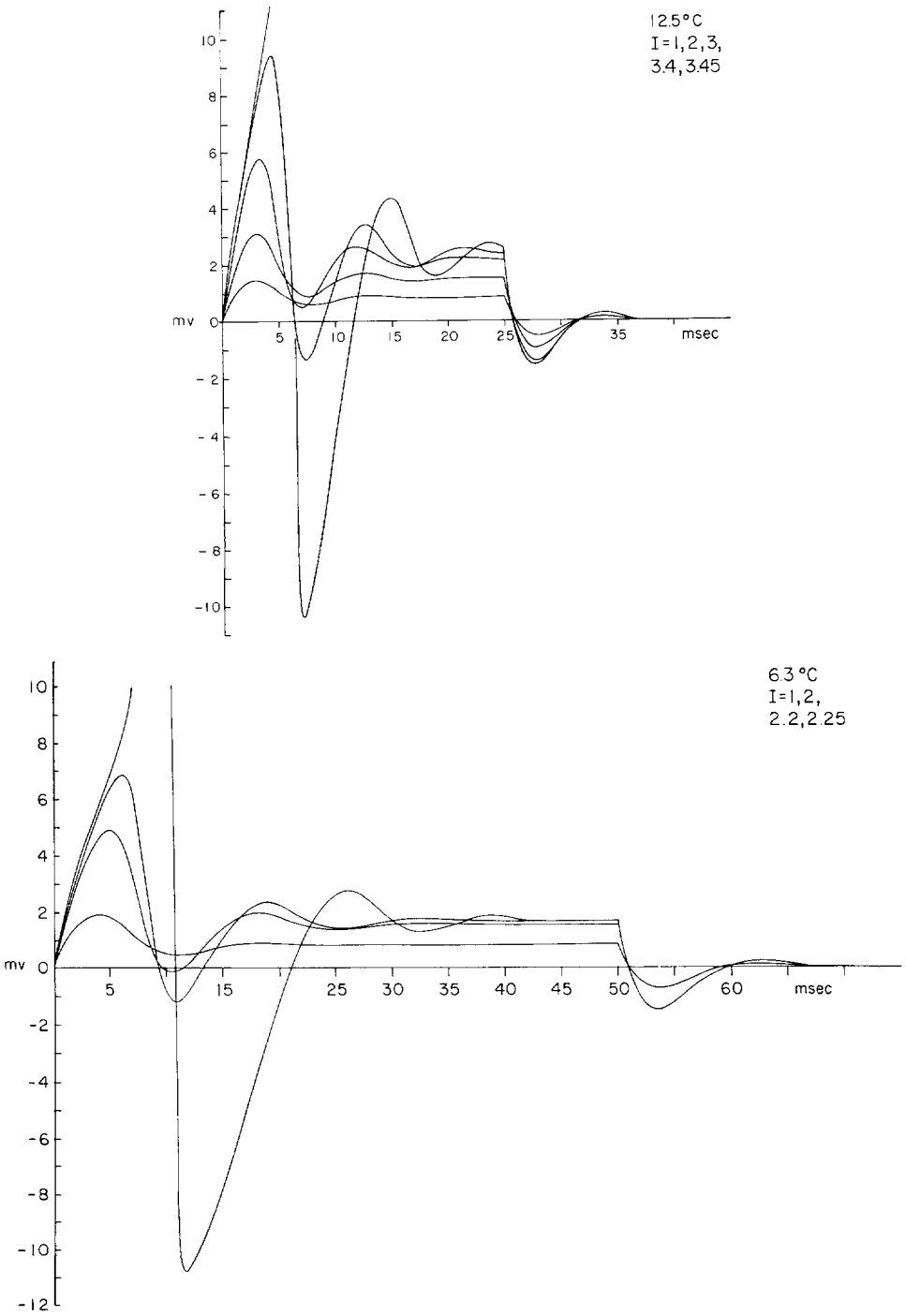

FIGURE 10. Computed responses for standard axon extending throughout the entire subthreshold regime, including the action potential. (Note, in the upper figure the downward stroke of the action potential was not included in the plot.) Current in μamp/cm^2. Compare upper figure with experimental tracings given in Fig. 6.

By collating data obtained on a series of axonal preparations Hodgkin and Huxley arrived at a set of "standard data" (Hodgkin and Huxley, 1952). These data were used for the computations[5] which are reported in this paper.

Small-Signal Range Computed responses in the small-signal range were obtained for three temperatures; namely, 6.3°, 12.5°, and 18.5°C. As prescribed in the paper of 1952 by Hodgkin and Huxley based upon analysis of temperature data, a Q_{10} of 3 (threefold change per 10°) was used to adjust the rate constants, α and β, of the time-variant conductances. The plotted results in Fig. 8 show clearly the oscillatory nature of the computed responses for a constant current stimulus. The symmetry of the response for a depolarizing and a hyperpolarizing current and the inverse temperature-dependence of the amplitude and period of the oscillation are also evident. These features are in good agreement with the experimental results as seen in Fig. 2.

The computed small-signal response with the membrane hyperpolarized to 12 mv, by a previously applied hyperpolarizing current is seen in Fig. 9. The RC response is clearly evident and contrasts with the oscillatory behavior occurring at the resting potential (cf. Fig. 3).

Quasi-Small-Signal When the computations are extended to higher currents, it is interesting to note (Fig. 10) that the oscillatory response is maintained with a moderate increase in the frequency as is seen in the experimental results (see Figs. 4 and 5).This property is displayed clearly in the computed results plotted; the temperatures, 6.3° and 12.5°C, were chosen as representative of the experimental range of temperature. Although suprathreshold behavior of the squid axon is not the primary concern of this communication, it is instructive to point out the correspondence between the experimental and computed response of the afterpotential; i.e., the undershooting and recovery of the membrane potential following an action potential. Compare the experimental recording in Fig. 6 with the computed response in Fig. 10 (upper).

Analysis and Discussion

A distinctive feature of the small-signal response—which is clearly confirmed in the computed response based on the three-current system—is the damped oscillatory excursion of the membrane potential upon both the application and the removal of a constant current. However, if the membrane is hyperpolarized to a certain level of potential the familiar RC response is observed. Although experimental data have not been presented here it will suffice to mention that at a further hyperpolarized level of membrane potential the RC response may even show an increase in the "capacitive" component of the

[5] Part of the computations were carried out by the method outlined in the monograph of Cooley and Dodge (Cooley, J., and F. Dodge. 1965. I.B.M. Research report RC-1496) and the remainder by a Runge-Kutta method.

membrane impedance. The additional "capacitance" acting in parallel with the membrane capacitance is a pseudocapacitance which arises from the same mechanism underlying the "inductive" component responsible for the oscillatory behavior appearing at the relatively depolarized state. We shall now treat in detail how a phenomenological[6] inductance or capacitance arises in the squid giant axon from time-variant resistance.

In the resting state, i.e. at the resting membrane potential $V = 0$, the magnitudes of the currents and conductances for a unit area of the "standard" axon are given in Fig. 11.

In order to emphasize the essential points in the analysis of the small-signal

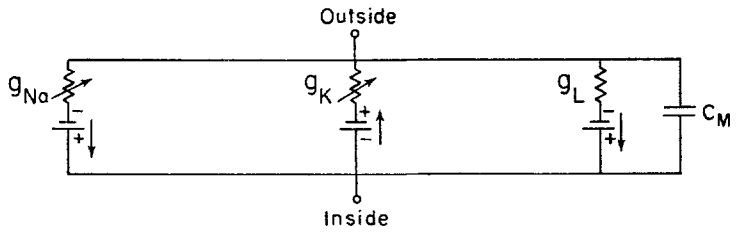

FIGURE 11. The electrical circuit representing the three-current system in the squid giant axon. The polarities of the individual emf's and the magnitudes of the respective resting currents and conductances are given below. Note the leakage conductance, g_L, is time-invariant.

$V_{Na} = 115$ mv	$V_K = -12$ mv	$V_L = 10.59$
$I_{Na_0} = -1.22 \times 10^{-6}$ amp/cm^2	$I_{K_0} = 4.39 \times 10^{-6}$	$I_L = -3.17 \times 10^{-6}$
$g_{Na_0} = 0.01 \times 10^{-3}$ mhos/cm^2	$g_{K_0} = 0.36 \times 10^{-3}$	$g_L = 0.3 \times 10^{-3}$
		$C_M = 1$ μFd/cm^2

behavior, it is convenient to consider only two currents, the potassium and the leakage current. That is, we shall consider both the sodium conductance, g_{Na}, and the membrane capacitance, C_M, to be zero. Before proceeding with an analytical treatment it may be instructive to describe graphically the response of the potassium time-variant conductance to a small step of current ΔI in the I, V plane. Fig. 12 is an expanded plot of the *steady-state* I, V characteristic of a system that qualitatively displays the electrical properties of the potassium system in the squid axon membrane.

If the membrane potential is at V_K (the emf of the potassium system) a small perturbation with a depolarizing constant current pulse ΔI, applied by means of current electrodes, will give rise to a sudden excursion from a to b along the slope of the I, V locus. (It is convenient to consider a relatively high re-

[6] Cole, by means of AC impedance measurements discovered this phenomenon in the squid axon, and he termed it "anomalous" impedance (Cole and Baker, 1941 *a*, *b*; Cole, 1941, 1949).

sistance in the leakage system such that the leakage current behaves in effect as a constant current system. Thus the applied ΔI appears entirely as a change in I_K .) Accordingly, the resulting potential change with time, as seen on the right, is to a good approximation a step response, the peak amplitude given

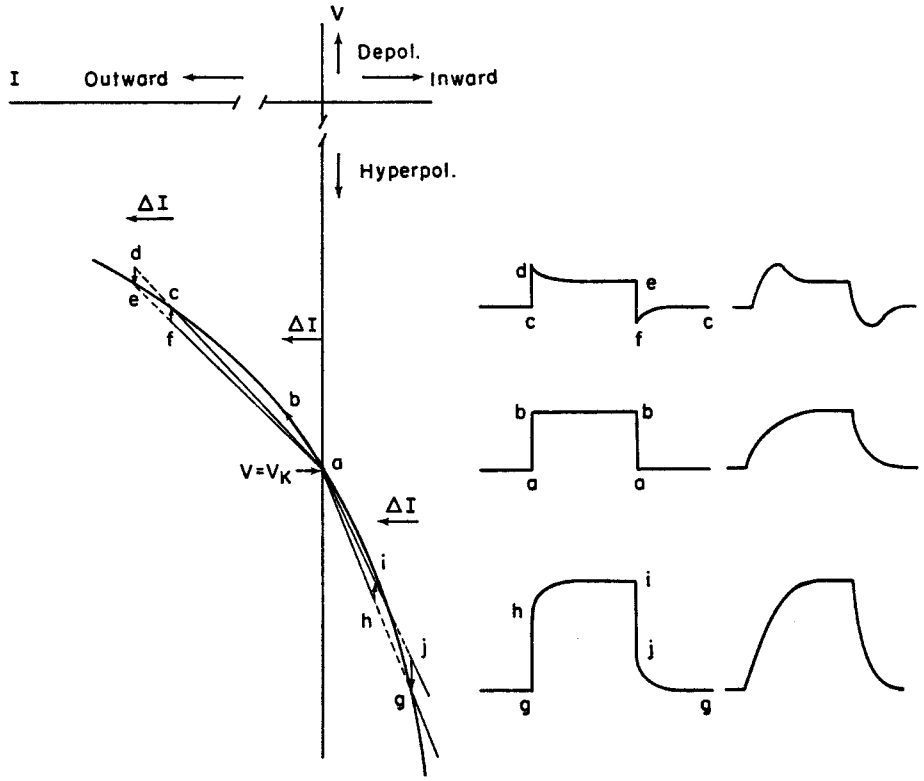

FIGURE 12. *I*, *V* steady-plot showing, qualitatively, the properties of the potassium current system in squid axon is seen on the left. Note, breaks are shown in the *I* and *V* axes to remind the reader that we are considering the *I*, *V* plot at a highly expanded scale in order to examine the "linear" (small-signal) response of ΔV with an applied ΔI. The response in time to a pulse of current ΔI at the different resting states, depicted by the points *c*, *a*, and *g*, is shown in the middle column. To the extreme right the corresponding response is shown when the membrane capacitance is added in parallel.

by the product of the slope resistance at $V = V_K$ and ΔI. Note at $V = V_K$ the slope resistance and the chord resistance are identical.

Proceeding to a depolarized level of potential as indicated by *c*, the *resting current is now nonzero*; namely, I_{K_0} . In this instance a constant current depolarizing pulse, ΔI, will drive the potential *suddenly* from *c* to *d* along the path given by the chord resistance. However, since the resistance is time-variant, the resistance will *decrease* continuously with time, as indicated by the trajec-

tory *d* to *e*, to approach the new steady-state resistance. Along the time axis the variation of the potential is seen to rise instantaneously and to fall off gradually resulting in a response with an inductive component. Upon termination of the current ΔI the potential falls suddenly along the trajectory *e* to *f*. Note, however, the *resting current*, I_{K_0}, is present and thus again, as a consequence of the time-variant resistance, the potential relaxes with a time lag, along the path *f* to *c*, returning to the initial steady-state condition at *c*. Along the time axis the potential displays undershooting and an asymptotic return to the resting state. Thus, the response is inductive both for the make and break of the applied pulse ΔI.

For a condition of hyperpolarization ($V < V_K$) as indicated by the point *g* on the *I*, *V* plot the response of the time-variant resistance to a depolarizing pulse, ΔI, can be traced in a similar manner. That is, with the onset of current, the potential rises suddenly from *g* to *h* along the path given by the chord resistance. However, due to the time-variant property of the resistance its magnitude must change; i.e., decrease with time, resulting in the movement along the trajectory *h* to *i*. At the end of the pulse, the potential falls suddenly along the path *i* to *j*, followed by a movement from *j* to *g* which requires finite time. It is readily seen that the response of the potential with time in this case has a capacitive component. It should be noted that the response is not symmetrical as reflected in the inequality of the trajectories, *h*, *i*, and *j*, *g*, and, accordingly, in the potential vs. time plot. This should serve to emphasize that the response of the system is basically asymmetrical and only in the limit, as ΔI approaches zero, can the system be considered as behaving linearly. In the trajectories, *d*, *e*, and *f*, *c*, discussed previously, the asymmetry is not so evident. ΔI in this instance gives rise to a variation in the state of the system which satisfies to a better approximation the condition of linearity.

The significant point which must be stressed with regard to the mechanism underlying the responses discussed is the fact that the potential of the system due to the emf is modified by the "IR" drop which of necessity must lag in time as a consequence of the time-variant nature of the resistance. *The potential variation arises solely from the change in resistance since the emf is strictly time-invariant.*

To the extreme right in Fig. 12 the responses are shown qualitatively for the three respective cases when the capacitance of the membrane C_M is included. For the depolarized state the pseudoinductance combines with the membrane capacitance to give a damped oscillatory response. In the hyperpolarized state the pseudocapacitance acts to augment the membrane capacitance.

Computations carried out with the standard data for the conditions discussed above for the two-current system (i.e. the potassium and leakage current) are seen in Fig. 13. With a constant current pulse of 1 μamp, for the condition $V > V_K$, the membrane potential clearly shows the pseudoinductive oscillatory behavior. Note that the damped oscillatory response is sym-

metrical with respect to the "on" and "off" of the current both for a depolarizing and a hyperpolarizing current.

At $V = V_K$ the pure RC response is evident as we should expect since the resting current is zero and therefore the effect due to time variation of the resistance is no longer present. It is at this level of membrane potential that the "electrotonic response" is displayed by the membrane.

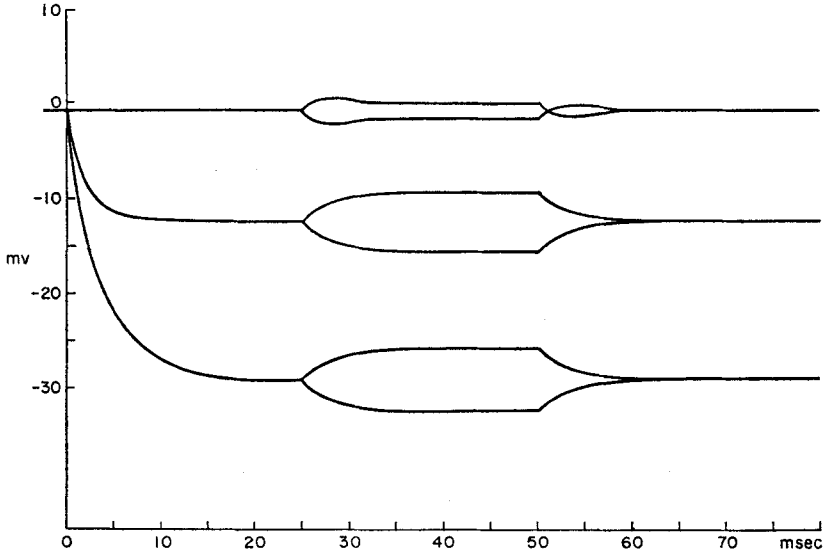

FIGURE 13. Computed response of the two-current system in the standard axon; i.e., the sodium conductance was set to zero. The levels of hyperpolarization and the corresponding hyperpolarizing currents are given in the legend of Fig. 9. The perturbing pulse was 1 μamp/cm^2. Note that as a consequence of setting the sodium conductance to zero and thus eliminating the sodium current the resting potential is hyperpolarized to -0.87 mv. Temperature, 6.3°C.

The pseudocapacitive response for levels of membrane potential $V < V_K$ is *not apparent since this effect is masked by the relatively low value of leakage resistance.* It should be noted that in the graphical analysis we eliminated the shunting of the leakage resistance (Fig. 12) by choosing a condition of constant current in the "leakage" system and thus were able to demonstrate the pseudocapacitive behavior.

Analytical Treatment

Small-Signal Phenomenological Impedance due to K System We shall now present the analytical expressions of the phenomenological impedance function based on the algebraic functions used by Hodgkin and Huxley as a reasonable empirical fit to the experimental data which they obtained for the potassium time-variant conductance. Thus for the two-current case which we have been

discussing, the total current, I, is given by

$$I = I_K + I_l$$
$$= g_K(V - V_K) + g_l(V - V_l)$$

where g_K and g_l are the potassium and leakage conductances, respectively. The time-variant conductance of the K system, g_K, was found to increase with time for a depolarizing step in the membrane potential, and conversely for a hyperpolarizing step. This experimentally observed characteristic was fitted adequately by (*a*) choosing a dimensionless variable, n, subject to a first-order diffential equation with time and (*b*) raising the resulting exponential function to the fourth power (see page 509 in Hodgkin and Huxley, 1952). Thus

$$g_K = \bar{g}_K n^4$$

where $\bar{g}_K$ is the maximum attainable conductance and $0 \leq n \leq 1$.

Accordingly,

$$I = \bar{g}_K n^4(V - V_K) + g_l(V - V_l).$$

Consider a variation in I, V, and g_K at a given steady state. Retaining only first-order terms and thereby linearizing the function describing the potassium conductance, we have that

$$\delta I = \bar{g}_K n_V^4 \delta V + 4\bar{g}_K n_V^3 (V - V_K)\delta n + g_l \delta V$$

where n_V is the steady-state value of n at the potential V (designated as n_∞ in Hodgkin and Huxley's notation).

Let us consider only the potassium current. We can eliminate the term δn as follows: Since the dimensionless variable, n, as already mentioned, is given by

$$\frac{dn}{dt} = \alpha_n(1 - n) - \beta_n n,$$

where α_n and β_n (established empirically from the experimental data) are solely functions of V, we have also that

$$\frac{d\delta n}{dt} = \delta\alpha_n - \alpha_n \delta n - n\delta\alpha_n - \beta_n \delta n - n\delta\beta_n.$$

Moreover, since α_n and β_n are solely functions of V, it is evident that

$$\delta\alpha_n = \left(\frac{d\alpha_n}{dV}\right)_V \delta V \quad \text{and} \quad \delta\beta_n = \left(\frac{d\beta_n}{dV}\right)_V \delta V$$

Thus

$$\frac{d\delta n}{dt} = \left(\frac{d\alpha_n}{dV}\right)_V \delta V - (\alpha_n + \beta_n)\delta n - n_V \left(\frac{d\alpha_n}{dV}\right)_V \delta V - n_V \left(\frac{d\beta_n}{dV}\right)_V \delta V$$

or

$$(p + \alpha_n + \beta_n)\delta n = \left[\left(\frac{d\alpha_n}{dV}\right)_V - n_V \left(\frac{d(\alpha_n + \beta_n)}{dV}\right)_V\right] \delta V$$

where $p \equiv d/dt$.

Finally

$$\delta I_K = \delta V \left[\bar{g}_K n_V^4 + 4\bar{g}_K n_V^3 (V - V_K) \left\{\frac{\left(\frac{d\alpha_n}{dV}\right)_V - n_V \left(\frac{d(\alpha_n + \beta_n)}{dV}\right)_V}{p + \alpha_n + \beta_n}\right\}\right].$$

Whereupon it is seen that δI_K is made up of two components

$$\delta I_K' = \delta V \bar{g}_K n_V^4 \quad \text{and} \quad \delta I_K'' = \delta V \frac{a}{p + b}$$

where

$$a \equiv 4\bar{g}_K n_V^3 (V - V_K) \left[\left(\frac{d\alpha_n}{dV}\right)_V - n_V \left(\frac{d(\alpha_n + \beta_n)}{dV}\right)_V\right]$$

and $b \equiv \alpha_n + \beta_n$. Since the observations we have been discussing have been obtained with constant current pulses, it may be more convenient to consider the "impedance" of the small-signal response, namely

$$\frac{\delta V}{\delta I_K'} = \frac{1}{\bar{g}_K n_V^4} \quad \text{and} \quad \frac{\delta V}{\delta I_K''} = \frac{1}{a} p + \frac{b}{a}.$$

Whereupon we can identify the parameters, R_K, r_n, and L_n, by

$$R_K = 1/\bar{g}_K n_V^4$$

$$r_n = \frac{b}{a} = \frac{\alpha_n + \beta_n}{4\bar{g}_K n_V^3 (V - V_K)\left[\left(\frac{d\alpha_n}{dV}\right)_V - n_V \left(\frac{d(\alpha_n + \beta_n)}{dV}\right)_V\right]}$$

$$L_n = \frac{1}{a} = \frac{r_n}{\alpha_n + \beta_n}.$$

Thus for a small-current perturbation the K system responds *as though* the

chord resistance, R_K (ohm cm²), were shunted by a series combination of a resistance r_n (ohm cm²) and an inductance L_n (ohm sec cm² ≡ henry cm²).

In terms of an equivalent circuit the impedance of the K system is clearly that seen in Fig. 14. In order to obtain the total impedance of the two-current system another resistance must be added in parallel due to the leakage system; namely, $R = 1/g_l$.

It is instructive to see how the explicit expression for the small-signal impedance agrees with the qualitative graphical analysis presented above: by examining the slopes of α_n and β_n, and n as a function of V (Hodgkin and

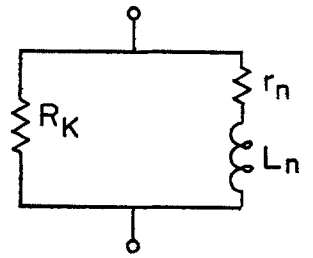

FIGURE 14. Equivalent circuit for the phenomenological impedance of the K system. R_K is the chord resistance.

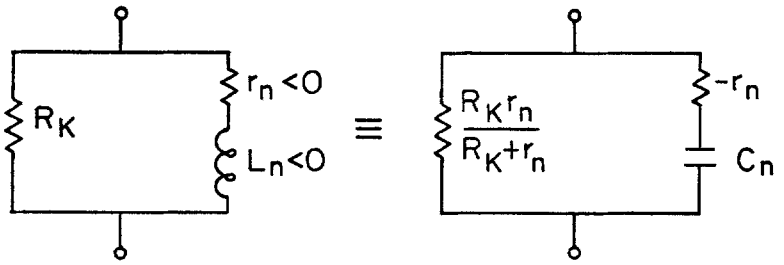

FIGURE 15. Equivalent circuit for the phenomenological impedance of the K system when the membrane potential is less than V_K. The negative inductance, L_n, transforms to a positive capacitance, C_n.

Huxley, page 511) it is seen that the term in brackets appearing in the denominator is a positive quantity. Note also that $V_K < 0$; i.e., -12 mv. Thus for depolarized levels of the membrane potential, i.e. $V > V_K$, both r_n and L_n are positive. As $V \to V_K$ both r_n and $L_n \to \infty$ which implies that the phenomenological impedance reduces to a pure resistance, $1/\bar{g}_K n_V^4$. However, for "hyperpolarized" levels, i.e. $V < V_K$, both r_n and L_n take on negative values. For convenience the latter can be readily transformed to an equivalent set of quantities in terms of a resistance and a capacitance in series, shunted by a resistance (Fig. 15). The equivalence between the two circuits can be established by satisfying three boundary conditions.

1. As the frequency approaches zero, the resistive component of the new circuit must be equal to that of the "basic" circuit which, by inspection, is clearly $R_K r_n/(R_K + r_n)$ (slope resistance).

2. As the frequency approaches infinity, the resistive component must reduce to R_K (chord resistance). Thus the resistance in the capacitive branch must be equal to $-r_n$.
3. The time constants of the reactive arms must be equal, namely,

$$\frac{L_n}{r_n} = -r_n C_n \quad \text{or} \quad C_n = -\frac{L_n}{r_n^2}.$$

It is evident that the "R, L" circuit for $V > V_K$ and the "R, C" circuit for $V < V_K$ will give rise to the transient responses which we established by means of the graphical analysis presented in Fig. 12. In order to emphasize the phenomenological nature of the elements, L_n and C_n, it should be noted that as $V \to V_K$, both r_n and L_n approach infinity and C_n approaches zero whereupon in either case the "reactive" current vanishes and the impedance is determined solely by R_K.

It is possible, if certain conditions are satisfied, to encounter for $V < V_K$ a region of the I, V characteristic in which the slope resistance $[R_K r_n/(R_K + r_n)]$ is negative. This facet of the I, V characteristic warrants discussion since the property of negative slope resistance (or, negative slope conductance) is one which may arise in general and, moreover, which plays a crucial role in the Na conductance. The conditions for the negative slope resistance can be shown readily by considering the macroscopic law of current

$$I = g(V - E)$$

where g is a function of V, and E is the emf of the system.

Differentiating with respect to V we have

$$\frac{dI}{dV} = \frac{dg}{dV}(V - E) + g.$$

Thus the slope conductance, at a given value of the conductance, g, can have a negative value in the region $V < E$ if $\frac{dg}{dV}$ is sufficiently "steep." Moreover, for increasing positive values of the emf the negative slope conductance increases in magnitude. In order to illustrate this important analytical property of a voltage-dependent conductance with which there is associated an emf the I, V characteristic of the K system of the standard axon was computed for different values of the emf (V_K). The results are given in Fig. 16. The emergence of the negative slope region as the emf (V_K) takes on more positive values is strikingly evident. Indeed even for $V_K = -12$ mv, a region of negative slope exists such that the quantity $R_K \cdot r_n/(R_K + r_n)$ is negative. This is not apparent in Fig. 16 since the current scale chosen to accommodate the entire set of data is much too coarse to indicate currents in the range of 0.02

μamp/cm^2 where the negative slope occurs. As is seen from Fig. 19 *a* the slope resistance is negative for $V < -15$ mv since $r_n < 0$ and $|r_n| < R_K$. Thus in this region the small-signal impedance of the potassium time-variant conductance is given by the negative slope resistance in parallel with a resistance $(-r_n)$ and a capacitance (C_n) in series.

Small-Signal Phenomenological Impedance due to Na System The small-signal properties of the Na system can be expressed analytically in a similar manner.

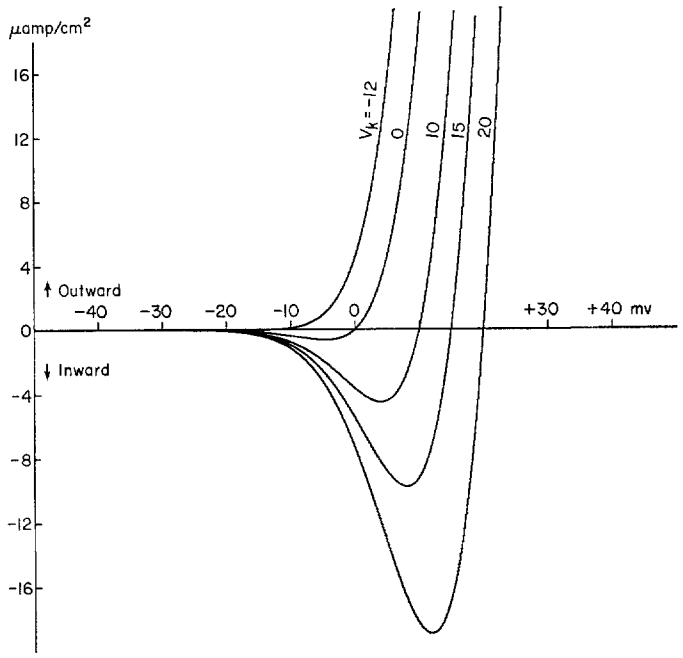

FIGURE 16. *I, V* steady-state plots of potassium current system in the standard squid axon for different values of the emf, V_K. Note the marked enhancement of the negative slope region with increasing values of V_K.

In this case from the analysis of the experimental data the time-variant conductance was found to have a rising and falling behavior for a depolarizing step in the membrane potential; i.e., "activation" and "inactivation" of the sodium time-variant conductance, respectively. Hodgkin and Huxley fitted this characteristic by postulating two dimensionless variables, m and h, which, as for the n variable of the K system, are subject to a first-order differential equation in time. Accordingly m, designated as the activation variable, must be an exponential increasing with time and h, the inactivation variable must be an exponential decreasing with time. An adequate fit to the experimental

data was obtained by raising m to the third power and multiplying by h to the first power. Thus the Na current is described by

$$I_{Na} = \bar{g}_{Na} m^3 h (V - V_{Na})$$

where $\bar{g}_{Na}$ is the maximum attainable conductance.

Again taking variations and retaining only first-order terms we have

$$\begin{aligned}\delta I_{Na} = {} & 3\bar{g}_{Na} m_V^2 h_V (V - V_{Na}) \delta m \\ & + \bar{g}_{Na} m_V^3 (V - V_{Na}) \delta h \\ & + \bar{g}_{Na} m_V^3 h_V \delta V.\end{aligned}$$

When the variational variables, δm and δh, are eliminated by following the same procedure as in the K system, we have

$$\begin{aligned}I_{Na} = {} & \delta V \bar{g}_{Na} m_V^3 h_V + 3\bar{g}_{Na} m_V^2 (V - V_{Na}) \frac{\left(\frac{d\alpha_m}{dV}\right)_V - m_V \left(\frac{d(\alpha_m + \beta_m)}{dV}\right)_V}{p + \alpha_m + \beta_m} \\ & + \bar{g}_{Na} m_V^3 (V - V_{Na}) \frac{\left(\frac{d\alpha_h}{dV}\right)_V - h_V \left(\frac{d(\alpha_h + \beta_h)}{dV}\right)_V}{p + \alpha_h + \beta_h}\end{aligned}$$

where three components of δI_{Na} can be identified; i.e.,

$$\delta I_{Na} = \delta I'_{Na} + \delta I''_{Na} + \delta I'''_{Na}.$$

Again, since we have been considering the application of current pulses to the axon, it is convenient to convert to impedance. Proceeding as in the case of the K system, it is evident that the small-signal phenomenological impedance is given by three components in parallel:

$$\frac{\delta V}{\delta I'_{Na}} = \frac{1}{\bar{g}_{Na} m_V^3 h_V} = R_{Na},$$

$$\frac{\delta V}{\delta I''_{Na}} = L_m p + r_m$$

and

$$\frac{\delta V}{\delta I'''_{Na}} = L_h p + r_h$$

where

$$r_m = \frac{\alpha_m + \beta_m}{3\bar{g}_{Na} m_V^2 h_V (V - V_{Na}) \left[\left(\frac{d\alpha_m}{dV} \right)_V - m_V \left(\frac{d(\alpha_m + \beta_m)}{dV} \right)_V \right]}$$

$$L_m = \frac{r_m}{\alpha_m + \beta_m},$$

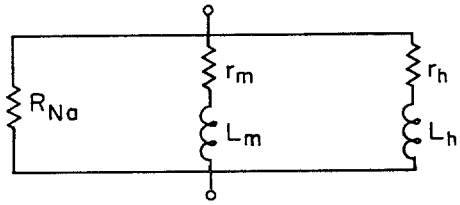

FIGURE 17. Equivalent circuit for the phenomenological impedance of the Na system. R_{Na} is the chord resistance.

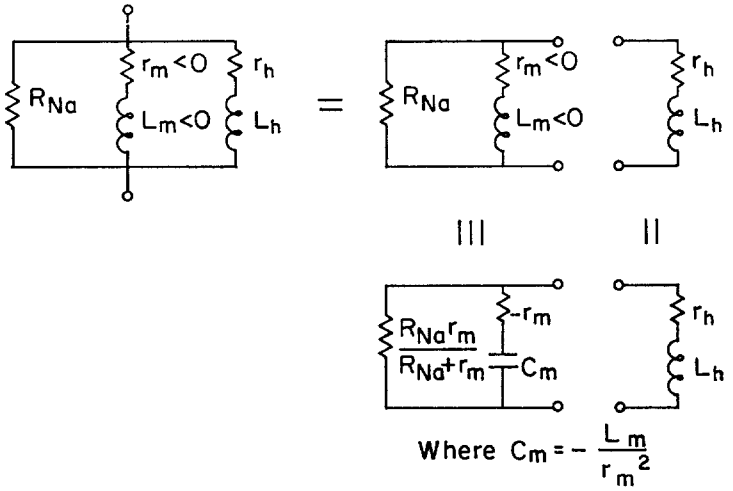

FIGURE 18. Equivalent circuit for the phenomenological impedance of the Na system when the membrane potential is less than V_{Na}. The negative inductance, L_m, transforms to a positive capacitance, C_m.

and

$$r_h = \frac{\alpha_h + \beta_h}{\bar{g}_{Na} m_V^3 (V - V_{Na}) \left[\left(\frac{d\alpha_h}{dV} \right)_V - h_V \left(\frac{d(\alpha_h + \beta_h)}{dV} \right)_V \right]}$$

$$L_h = \frac{r_h}{\alpha_h + \beta_h}.$$

In this case two R L elements appear, one reflecting the rising and one the

falling behavior of the time-variant conductance. Expressed by means of an electric circuit the small-signal impedance is given in Fig. 17. Upon examining the values of α_h, β_h, $\frac{d\alpha_h}{dV}$, and $\frac{d\beta_h}{dV}$ as a function of V it is seen that the term

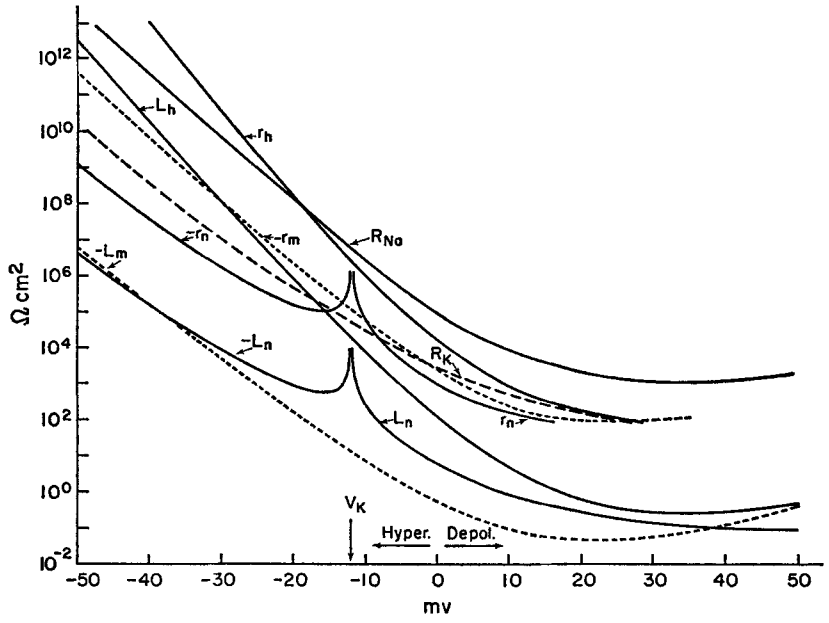

FIGURE 19 *a*. Computed values of the parameters, r_n, L_n, r_m, L_m, r_h, L_h, R_{Na}, and R_K as a function of V for $V_K = -12$ mv and $V_{Na} = 115$ mv. Temperature, 6.3°C. Note, although not indicated, the unit for inductance is henry cm².

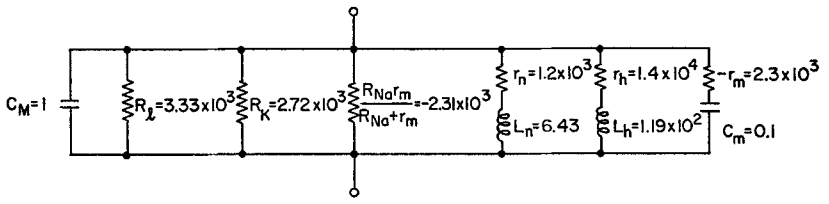

FIGURE 19 *b*. Equivalent circuit for the total membrane impedance at the resting membrane potential ($V = 0$). Temperature, 6.3°C. Resistance is given in ohm cm², capacitance in μFd/cm², and inductance in henry cm².

in brackets appearing in the denominator of the expression for r_h (and L_h) is a negative quantity. Note that $V_{Na} > 0$; i.e., 115 mv. Thus for $V < V_{Na}$, which is the only condition of interest, since either the condition $V = V_{Na}$ or $V > V_{Na}$ is rarely attained, both r_h and L_h are positive. However, a similar examination for the m variable indicates that r_m and L_m take on negative

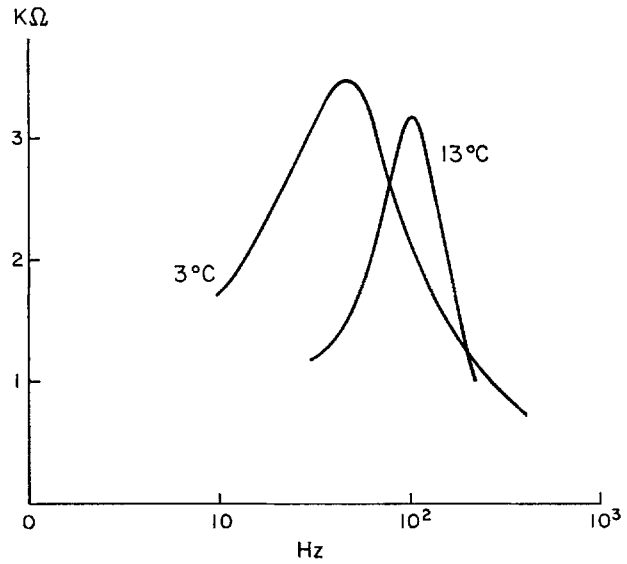

FIGURE 20 *a*. Small-signal response of squid axon to variable frequency alternating current ("constant current" source). Note resonance and the dependence of resonant frequency on temperature. The values along the ordinate are given by the ratio of the peak voltage to the peak current for a 2 cm length of axon.

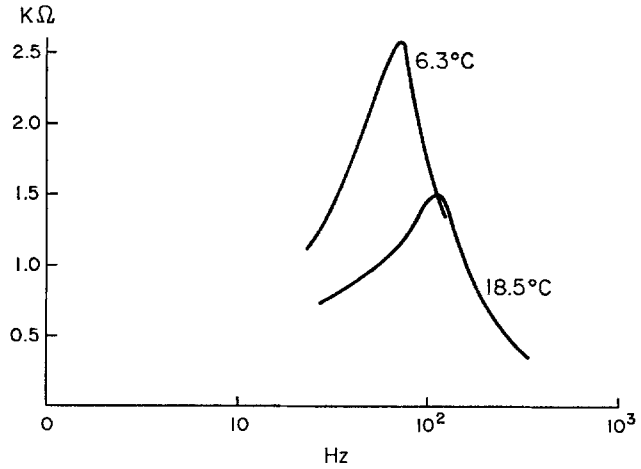

FIGURE 20 *b*. Computed small-signal response of standard axon to AC current. The values along the ordinate are given by the ratio of the peak voltage to the peak current for 1 cm^2 of axonal membrane.

values. Thus as we demonstrated in our discussion of a similar condition arising in the K system ($V < V_K$), the negative values of r_m and L_m can be converted to a set consisting of a resistance and capacitance in series, shunted by a resistance. Upon considering R_{Na} in combination with r_m, L_m it is evident that

we can obtain an equivalent R, C system (Fig. 18). The equivalent circuit of the total impedance is shown in Fig. 19 *b* with the values for the resting membrane potential at $V = 0$ obtained from a calculation of the parameters r_n, L_n, r_m, L_m, r_h, L_h, R_{Na}, and R_K, as a function of V ($V_K = -12$ mv and $V_{Na} = 115$ mv, at 6.3°C). A plot of these results is given in Fig. 19 *a*. Thus, in general, we have four reactive elements appearing in the total impedance, three of which are phenomenological due to the potassium and sodium time-variant conductances and the fourth, a conservative element, due to the membrane capacitance. The negative resistance element (-2.31×10^3 ohms) arises as a consequence of the fact that in the range of $V = 0$ the I, V characteristic of the Na system has a negative slope resistance.

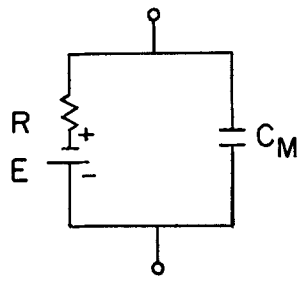

FIGURE 21. Equivalent circuit of classical single-current system postulated to explain electrotonus.

Since the total impedance is in essence a parallel "R L C" configuration,[7] the phenomenon of parallel resonance should be obtained with an alternating current applied to the membrane. Indeed this behavior is well-documented in the impedance measurements of Cole and others. In Fig. 20 *a* data are presented which were obtained on a giant axon of *Loligo vulgaris* at two different temperatures, 3° and 13°C. The computed response is seen in Fig. 20 *b*. It will suffice here to mention merely that the amplitude at resonance increases as the temperature is lowered. This is, of course, consistent with the transient response to a step of current discussed previously.

In order to more fully appreciate the physiological implications of the three-current system, it is instructive to consider the small-signal properties of the classical single-current system which was introduced by Hermann to explain the spread of demarcation potentials and electrotonus in nerve fibers. As seen in Fig. 21 the single-current system must of necessity have a zero resting current and thus the membrane potential must be equal to the emf. This condition corresponds to the case $V = V_K$ discussed above for the "K system" and, accordingly, in the single-current system the response to a small per-

[7] The fourth-order linear differential equation which describes the small-signal behavior of the three-current system has a single pair of complex conjugate roots and two real negative roots [cf. Fig. 7 (right) in Cooley et al., 1965]. See table in Appendix for computed values of frequency (given by the imaginary part of the conjugate roots) in the subthreshold range $V = 0$ to $V = 9$, for 6.3°, 12.5°, and 18.5°C.

turbation, ΔI, must be purely resistive. It is important to emphasize that if inductive or capacitive responses were to occur in the single-current system they would arise solely from a time-variant emf, in sharp contrast to the mechanism of phenomenological impedance which arises solely from a time-variant conductance—a dissipative element—operating in conjunction with a finite resting current due to the existence of two or more currents in the membrane. It is certainly possible that a single-current system could be operating in an excitable membrane but it must be clearly understood that if this were the case a *change in emf would be absolutely necessary* to generate either small-signal or large-signal responses. In the squid giant axon the experimental evidence points to the fact that at least three systems of electric current are present in the axonal membrane and that the emf in each system is time-invariant, in which case both the small- and large-signal responses arise exclusively from the voltage-dependent, time-variant conductances.

APPENDIX

TABLE

COMPUTED VALUES OF FREQUENCY OF FOURTH-ORDER LINEAR DIFFERENTIAL EQUATION FOR STANDARD AXON

Membrane potential V	Frequency in hertz		
	18.5°C	12.5°C	6.3°C
0	118.695	87.582	61.018
1	134.032	97.996	68.046
2	149.749	108.482	74.981
3	165.980	119.008	81.245
4	182.141	129.035	86.934
5	198.230	138.567	91.785
6	213.681	147.211	95.795
7	228.614	154.877	98.930
8	242.813	161.871	101.296
9	256.332	167.739	102.992

Received for publication 14 June 1969.

REFERENCES

ARVANITAKI, A. 1939. Recherches sur la réponse oscillatoire locale de l'axone géant isolé de *Sepia*. *Arch. Int. Physiol.* **49**:209.

ARVANITAKI, A. 1941–1943. Réactions au stimulus anodique étude de la réponse électrique locale de signe postif. Observations sur l'axone isolé de *Sepia*. *J. Physiol. Pathol. Gen.* **38**:147.

BRINK, F., JR., D. W. BRONK, and M. G. LARRABEE. 1946. Chemical excitation of nerve. *Ann. N. Y. Acad. Sci.* **47**:457.

CHANDLER, W. K., R. FITZHUGH, and K. S. COLE. 1962. Theoretical stability properties of a space-clamped axon. *Biophys. J.* **2**:105.

COLE, K. S. 1941. Rectification and inductance in the squid giant axon. *J. Gen. Physiol.* **25**:29.

COLE, K. S. 1949. Dynamic electrical characteristics of the squid axon membrane. *Arch. Sci. Physiol.* **3**:253.

COLE, K. S., and R. F. BAKER. 1941 *a*. Transverse impedance of the squid giant axon during current flow. *J. Gen. Physiol.* **24**:535.

COLE, K. S., and R. F. BAKER. 1941 *b*. Longitudinal impedance of the squid giant axon. *J. Gen. Physiol.* **24**:771.

CONTI, F., and G. PALMIERI. 1968. Nerve fiber behavior in heavy water under voltage clamp. *Biophysik.* **5**:71.

COOLEY, J., F. DODGE, and H. COHEN. 1965. Digital computer solutions for excitable membrane models. *J. Cell. Comp. Physiol.* **66**:99.

DAVIS, L., and R. LORENTE DE NÓ. 1947. Studies from The Rockefeller Institute for Medical Research. **131**. Chapter IX.

EYZAGUIRRE, C., and S. KUFFLER. 1955. Processes of excitation in the dendrites and in the soma of single isolated sensory nerve cells of the lobster and crayfish. *J. Gen. Physiol.* **39**:87.

FUORTES, M. G. F. 1958. Electric activity of cells in the eye of *Limulus*. *Amer. J. Ophthalmol.* **46**:210.

GUTTMAN, R. 1969. Temperature dependence of oscillation in squid axons: comparison of experiments with computations. *Biophys. J.* **9**:269.

HAGIWARA, S., and Y. OOMURA. 1958. The critical depolarization for the spike in the squid giant axon. *Jap. J. Physiol.* **8**:234.

HERMANN, L. 1905. Beitrage zur Physiologie und Physik des Nerven. *Arch. ges. Physiol.* **109**:95.

HODGKIN, A. 1938. Subthreshold potentials in a crustacean nerve fiber. *Proc. Roy. Soc. Ser. B Biol. Sci.* **126**:87.

HODGKIN, A. L., and A. F. HUXLEY. 1952. A quantitative description of membrane current and its application to conduction and excitation in nerve. *J. Physiol. (London).* **117**:500.

HODGKIN, A. L., and W. RUSHTON. 1946. The electrical constants of a crustacean nerve fibre. *Proc. Roy. Soc. Ser. B. Biol. Sci.* **133**:444.

HUXLEY, A. F. 1959. Ion movements during nerve activity. *Ann. N. Y. Acad. Sci.* **81**:221.

MAURO, A. 1961. Anomalous impedance, a phenomenological property of time-variant resistance. An analytic review. *Biophys. J.* **1**:353.

SABAH, N. H., and K. N. LEIBOVIC. 1969. Subthreshold oscillatory responses of the Hodgkin-Huxley cable model for the squid giant axon. *Biophys. J.* **9**:1206.